Vol. 20, No. 3(2021) Sim2453
Revista Mexicana de Ingeniería Química

Prediction and modeling of harmonic current behavior in grid-connected photovoltaic systems based on NARX networks

Predicción y modelado del comportamiento de corrientes armónicas en sistemas fotovoltaicos conectados a red basados en redes NARX

A.A. Jumilla-Corral[1], C. Pérez-Tello[1], H.E. Campbell-Ramírez [1], Z.Y. Medrano-Hurtado[2*], P. Mayorga-Ortiz[3]

[1]*Instituto de Ingeniería, Universidad Autónoma de Baja California, Mexicali, México.*
[2]*Departamento de Ciencias Básicas, Instituto Tecnológico de Mexicali, Mexicali, México.*
[3]*Departamento de Eléctrica-Electrónica, Instituto Tecnológico de Mexicali, Mexicali, México.*

Received: April 25, 2021; Accepted: July 25, 2021

Abstract

This research presents the modeling and prediction of the harmonic behavior of current in an electric power supply grid with integration of photovoltaic power by inverters. The methodology was based on the use of recurrent artificial neural networks of the nonlinear autoregressive with external input type. Data were obtained from experimental sources through the use of a test bench, measurement, acquisition and monitoring equipment. The input-output parameters for the neural network were the values of current in the inverter and in the supply grid respectively. Results shown that the neural network can capture the dynamics of the analyzed system. The generated model presented flexibility in data handling, representing and predicting the behavior of the harmonic phenomenon. The obtained algorithm can be transferred to a physical or virtual system, for the control or reduction of harmonic distortion.

Keywords: model, prediction, inverters, photovoltaic systems, artificial neural networks, nonlinear autoregressive with external input.

Resumen

Esta investigación presenta el modelado y predicción del comportamiento armónico de la corriente en una red de suministro eléctrico con integración de potencia fotovoltaica mediante inversores. La metodología se basó en el uso de redes neuronales artificiales recurrentes del tipo no lineales autorregresivas con entradas externas. Los datos fueron obtenidos de fuentes experimentales mediante el uso de un banco de pruebas, equipo de medición, adquisición y monitoreo. Los parámetros de entrada-salida para la red neuronal fueron los valores de corriente en el inversor y en la red de suministro respectivamente. Los resultados mostraron que la red neuronal puede captar la dinámica del sistema analizado. El modelo generado presentó flexibilidad en el manejo de datos, representando y prediciendo el comportamiento del fenómeno armónico. El algoritmo obtenido puede ser trasladado a un sistema físico o virtual, para el control o reducción de la distorsión armónica.

Palabras clave: modelo, predicción, inversores, sistemas fotovoltaicos, redes neuronales artificiales, red neuronal no lineal autorregresiva.

* *Corresponding author. E-mail*: zulmamh@itmexicali.edu.mx
https://doi.org/10.24275/rmiq/Sim2453
ISSN:1665-2738, *issn-e*: 2395-8472

1 Introduction

Renewable energies are considered clean, abundant and increasingly competitive. They differ from fossil fuels in their diversity, profusion and harnessing potential in all regions of the planet, and they do not generate greenhouse gases nor polluting emissions (Nadeem Javaid, 2018; M.D. Gomez, 2020).

Among renewable energy sources, photovoltaic energy (PV) is included, which involves the direct transformation of solar radiation into electrical energy, this transformation is achieved by leveraging the properties of semiconductor materials such as silicon, which can generate electrical power when ionized by solar radiation (Angèle Reinders, 2017; C. Álvarez, 2019).

PV generation systems are classified into two large groups: isolated and interconnected (Sunaina Singh, 2019). In the former, the generation is not connected in any way to the electric supply grid, in the latter, the energy generated is integrated into the grid by the use of electronic power inverters.

Inverters used in interconnected PV systems convert direct waveform power (DC) into sinusoidal alternating waveform power (AC) (Kumar Gupta, 2017). These devices due to the nonlinear behavior of their components and operational characteristics, generate power quality issues, such as transients and voltage variations, flickering, harmonics (voltages or currents with a frequency that is an integer multiple of the fundamental supply frequency -60/50 Hz-) and interharmonics (voltages or currents with a frequency that is a non-integral multiple of the fundamental supply frequency), (Bincy, 2017; Plangklang, 2016).

Harmonic distortion (voltage and current variations due to changes in frequencies within the electrical distribution systems), increases Joule effect losses (physical effect by which the pass of current through an electrical conductor produces thermal energy) in electric feeders, overheating in grounded conductors, motors, generators, transformers and cables, reducing their service life; vibration in electrical machines, failure of capacitor and transformer banks, resonance effects (electrical resonance occurs in an electric circuit at a particular resonant frequency when the impedances or admittances of circuit elements cancel each other), as well as operational problems in sensitive electronic devices and interference in telecommunications systems. (Yu-Wei Liu, 2018).

Due to the imminent growth in the use of PV systems interconnected to power grids, which have led to an increase in energy quality problems (Ariya Sangwongwanich, 2019), specifically those caused by harmonic distortion; need to characterize and model harmonic behavior due to the integration of the PV power is necessary, particularly to control and/or suppress the harmonic distortion at the common coupling point (CCP -the point where the Interconnection Facilities connect with the Utility's System-), as well as in the power supply grid.

Several researches show the modeling of harmonic behavior in electrical grids with power integration from PV generation systems, both in medium and low voltage (Nduka and Pal, 2017; Vargas, Ramirez and Lazaroiu 2017; Deng, Rotaru and Sykulski 2017; Todeschini, Balasubramaniam and Igic 2019). Artificial Neural Networks (ANN) have traditionally been used for detection, classification and control of energy quality problems, in particular those related to voltage and current harmonic distortion, as well as in systems that aim to control and/or eliminate such phenomena (Mubarok *et al*., 2017; Mejia-Barron *et al*., 2017; Rodriguez *et al*., 2019; Kumar and Panigrahi, 2019; Shukl and Singh, 2020). Recurrent Neural Networks (RNN) and diffuse interference have been used in the modeling and prediction of current harmonics injected into energy micro grids, by different types of loads (Hatata and Eladawy, 2017; Panoiu M.; Panoiu C.; Ghiormez L., 2018).

This paper shows the modeling and prediction of current behavior in a power grid under critical operating conditions, when the CCP integrates powers from this grid and a PV system, through a solid-state inverter, simultaneously powering resistive loads. The methodology used is based on the use of nonlinear autoregressive with external input (NARX), and the results may serve as a future guide for the control and/or suppression of harmonic content in the CCP of such systems.

ANN are computer algorithms that simulate the biological activity of neurons and the processing of human brain information (Alhroob *et al*., 2019). They are distinguished in fields of science where the conception of solutions or characteristics of problems analyzed, are difficult to determine with conventional programming, such as image and voice processing, pattern recognition, planning, adaptive interfaces for human/machine systems, control and optimization, signal filtering, modeling and prediction (Shrestha and Mahmood, 2019). According to their topology they are classified into monolayers, multilayers, convolutional,

radial-based and recurrent.

RNN do not have a layer structure (such as single-layer, multilayer, and convolutional networks), but allow arbitrary connections between neurons, even being able to create loops, thus establishing temporality, allowing the network to have memory (Rezk, *et al*., 2020). Data that enters at a time "t" to the entry of the network, are converted and transferred in it, even in the later moments of time, t+1, t+2, t+3…This architecture of neural networks has become a model implemented in different domains, due to its natural ability to process sequential inputs and know their dependencies in the long term (Xia *et al*., 2018). Unlike conventional ANN (forward), RNN are connected to each other in the same hidden layer and a training function is applied repeatedly to hidden states (Salas, Barros, and Martinez, 2019). RNNs are archetypes of deep learning, which are repeatedly fed back.

NARX networks have performed adequately in diverse applications, especially in sequential problems, as well as in dynamic system modeling and time series prediction (Li and Cao, 2018), (Cortez *et al*., 2018), (Liu, Chen and Wang, 2018). The equation that defines the NARX network model is:

$$y(t) = f[(y(t-1), y(t-2), \ldots y(t-ny), x(t), x(t-1), x(t-2), \ldots x(t-nx)] \quad (1)$$

where the next value of the dependent output signal y(t) is calculated from previous output signal values and previous values of the independent (external) input signal.

When applying a NARX network to a system, the end result to obtain a model for it. This is accomplished by using feedback (the output is fed back to the input) whether in a closed loop or in a parallel loop. By having such output available during the training phase of the network (the real output), other configurations can be achieved, such as the serial-parallel or the open loop one. This brings forth several benefits to the training phase. One such benefit is more precision on the input of the network and a feedforward orientation, which can be used to apply a static backpropagation (Hudson, Hagan, and Demuth, 2019; E. Figueroa, 2020; L. Díaz, 2020).

Fig. 1 shows an open-loop NARX network for modeling (a), while a closed-loop NARX network for prediction is shown in (b), were the Tapped Delay Line (TDL), is a memory structure formed of n buffers, were every oldest input is replaced by a new one, and each input takes part in the learning process per turn.

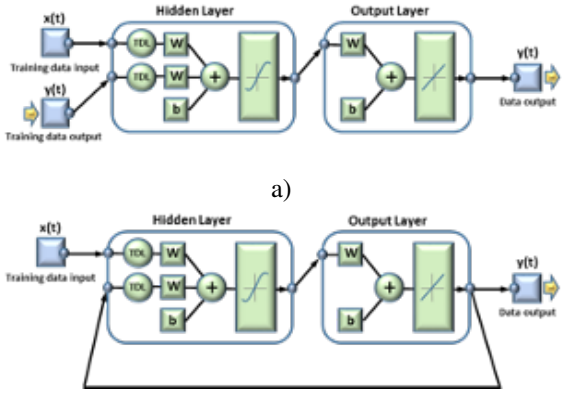

Fig. 1. NARX network architecture: (a) Open loop network (parallel-series); (b) Closed loop network (parallel).

2 Methodology and development

For modeling and prediction of current's behavior in a 220 V, 60 Hz electrical supply grid, where the powers of the electrical grid and a PV system are integrated through electronic inverters, a test bench was used. This test bench is comprised by six monocrystalline solar panels with a rating of 250 watts each, providing 1500 watts in total. A voltage controlled central inverter in full bridge mode with a power rating of 3000 watts at 220 volts is used. The PCC is located on a single phase, 220 volt, 100 amp electrical panelboard. Resistive loads rated at 530 watts for 127 volts are used for the model. To acquire the system's current, Hall Effect sensors (model ACS712) are used in conjunction with a National Instruments acquisition device (model NI USB-6008). The experimental methodology for data acquisition and modeling of dynamic system behavior using ANN is as follows:

1. Design and construction of the test bench,
2. Connection and configuration of acquisition equipment,
3. Data acquisition for references,
4. Data acquisition for modeling,
5. Determination of the ANN to be used,
6. Structure of the ANN to be used,

7. Application of ANN (training, validation and testing of ANN),

8. Results and conclusions.

Fig. 2 shows the arrangement of the test bench elements.

The phase conductors in each feeder (inverter and supply grid) were connected in series to the ACS712 current sensors, between their terminals: source (IP+) and load (IP-). With a polarization voltage of 5 Vdc between the Vcc and GND terminals of each sensor. Fig. 3 shows the connection of data acquisition devices.

Data acquisition of current was carried out in the network feeder for 5 seconds, without power inputs from the PV system, used a sample rate of 10,000 samples/second to obtain information about background harmonic distortion (harmonic distortion produced by external loads to the network under study), in the feeder. Data acquisition of the system´s current was done simultaneously in both feeders (supply grid and inverter), at CCP, with a sample rate of 5,000 samples/second for each feeder for 5 seconds. Table 1 shows the measurement points and signal acquisition conditions.

Fig. 4 shows the graphical representation time and magnitude parameters of supply grid signal, without inputs power from the PV system.

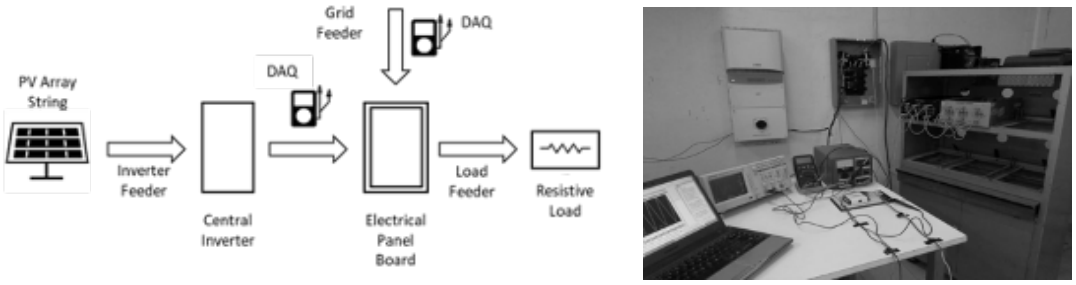

a) b)

Fig. 2. Arrangement of elements in test bench: a) Schematic diagram; (b) Physical arrangement of equipment.

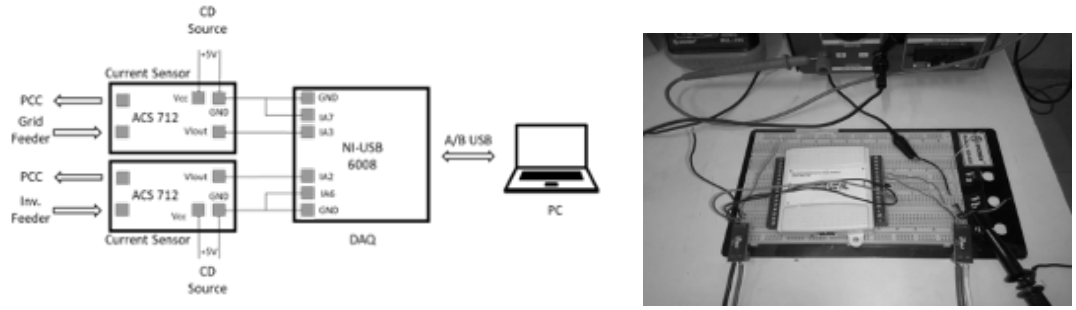

a) b)

Fig. 3. Connecting devices for data acquisition: (a) Schematic diagram; (b) Physical arrangement of data acquisition equipment.

Table 1. Description and conditions for data acquisition.

Data acquisition		
No.	Description	Conditions of acquisition
1	Supply grid feeder	No current input from the inverter and charging at CCP
2	Supply grid feeder	With input of current by the inverter and charging at CCP
3	Inverter feeder	With charging at CCP

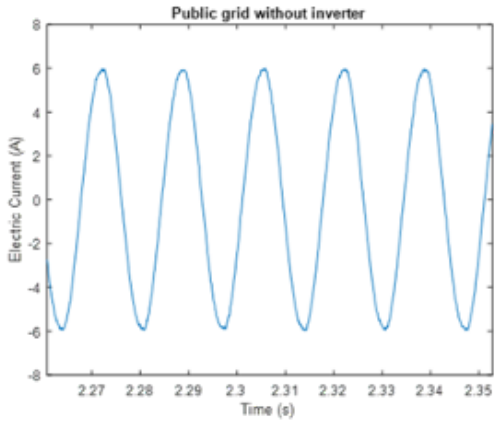

Fig. 4. Current in the grid feeder without inputs power from the PV system.

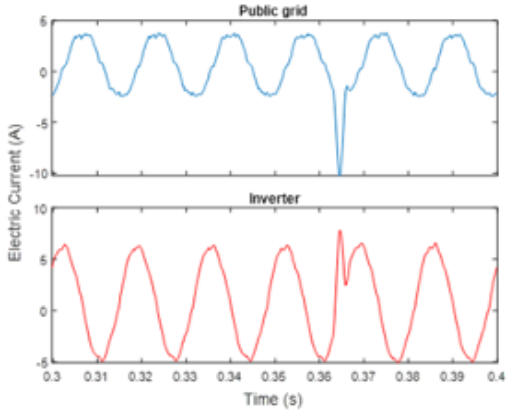

Fig. 5. Currents in supply grid and inverter, feeding a resistive load.

Fig. 4 shows a sinusoidal signal with a positive peak magnitude of 5.98 amps, with a small background harmonic distortion (1.07%), and non-dynamic (invariant in time) behavior. Fig. 5 corresponds to the current in both feeders (supply grid and inverter), simultaneously feeding resistive load. This graph shows the change in the waveform of the current signal in the supply grid after PV power integration. Both signals show distortion due to the presence of harmonics and nonlinear dynamic behavior.

Due one of the characteristics of ANNs is that of not having a single structure, a NARX networks configured with a series-parallel architecture (open loop), was used for the modeling network and in parallel (closed loop), for the prediction network, used to check the proper functioning of the resulting model (Hudson, Hagan, and Demuth, 2019). Both networks are powered by input signals at the start of the network,

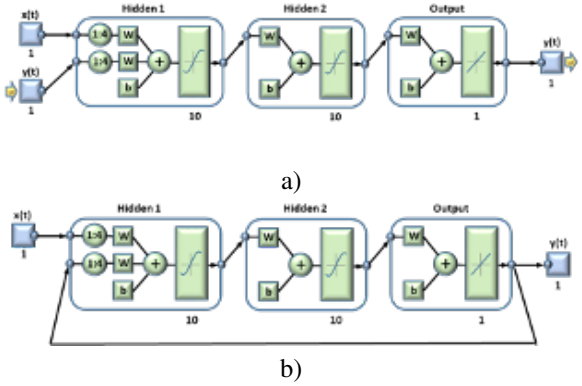

Fig. 6. Architecture of configured NARX networks: a) Serial-parallel architecture (open loop); b) Parallel architecture (closed loop).

containing two hidden layers with 10 neurons each, activated by sigmoid functions and an output layer with a single neuron activated by a linear function. Fig. 6 shows the structures of the NARX networks used. These networks have four variable offsets (shown by the 1:4 ratio in the Tapped Delay Line), this indicates that the input signals are made up of x(t), x(t-1), x(t-2), x(t-3) and x(t-4), and have input variables y(t-1), y(t-2), y(t-3) and y(t-4), for the series-parallel network; and z(t-1), z(t-2), z(t-3) and z(t-4), for the network in parallel, being "y" the actual output and "z" the estimated output.

NARX network training is supervised, giving the network input patterns, as well as expected output (correct result). The input and output data consist of vectors line of 1 by 25,000 elements each one, and correspond to the magnitudes of currents in the inverter feeder (input data) and the magnitudes of currents in the electrical supply grid (expected output). The Levenberg-Marquardt algorithm is used as a training method, along with the mean squared error (mse) performance function, with a total of a thousand iterations (epochs). The method used for calculating gradients was dynamic backpropagation.

The criteria for stopping training is defined by the number of epochs (1,000 iterations), gradient (less than 10^{-5}), and 6 as the number of validation checks.

The general procedure in both networks consisted of the introduction of inputs (where the input neurons are activated); then the information is propagated through the networks and outputs were generated; then the outputs of the networks are compared to the desired outputs and the errors are calculated; finally, corrections are made to the weights that are based on these errors until they were minimized.

During training, the dataset is randomly divided (to avoid an over fit effect), into three subsets for each network. The first subset was the training set. With this dataset network learning are carried out through weight adjustment and corresponded to 70% of the total data. The second subset (with 15% of the data), was the validation set that served to monitor the error during the training process. The last subset with the remaining 15% of the data are the test set, it was not used during training, but was subsequently used to evaluate network performance (Hudson, Hagan, and Demuth, 2019).

3 Results

After the parameterization of the series-parallel NARX network, this network was trained using the Levenberg-Marquardt method, using 269 iterations of the 1,000 available epochs to obtain the lowest performance value before stopping the algorithm, because 6 or more times there were no changes in that performance during testing with validation data. Fig. 7 exhibits a very fast drop in mse, before 10 iterations.

Fig. 7 shows how errors in training, validation, and test data follow the same trends during the algorithm execution; stopping when it gets an mse less than 10^{-2}. It also shows the minimum value of the network performance obtained in iteration 269, this being 0.067622.

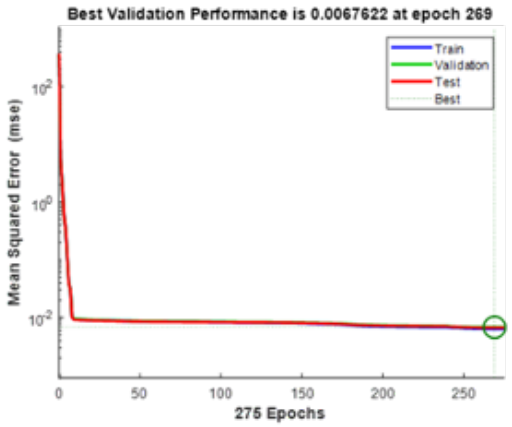

Fig. 7. Development of training, validation and testing, in relation with the number of iterations used, as well as the mse obtained.

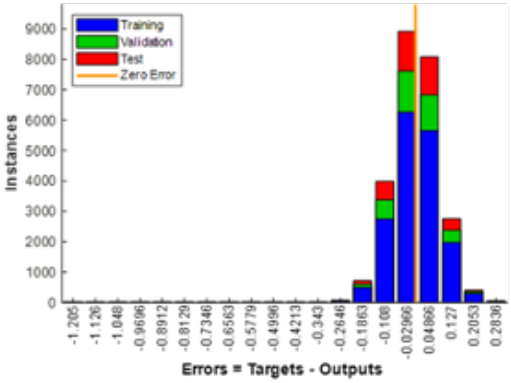

Fig. 8. Histogram of the error of outputs against target.

Fig. 8 shows the histogram containing the errors in the three datasets. It is determined that, on the center line, the data ratio of the training set is higher, and this behavior is constant during the analysis of the data furthest from the null error, while always retaining the higher proportion of the training data, in relation with the validation and test data. This trend observed in the behavior of the data shown in Fig. 7.

Linear regression is used to analyze the errors for each dataset (training, validation, and testing). Fig. 9 shows the values between the achieved output and the required targets. The best conditions being those of training data that have a 99.938% effectiveness in regression. This result can be attributed to a greater amount of data (70% of the total), with which the training was carried out. There is also a lot of proximity to the other data groups regarding the effectiveness of regression.

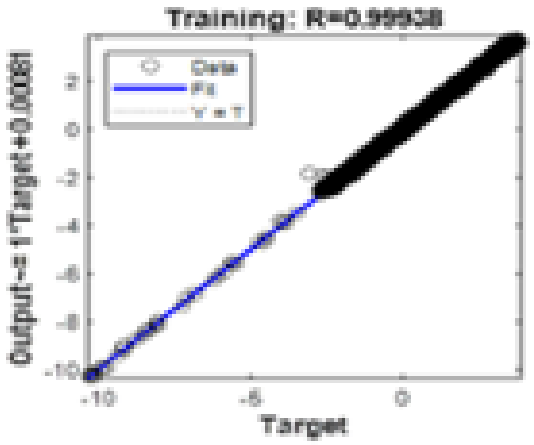

a)

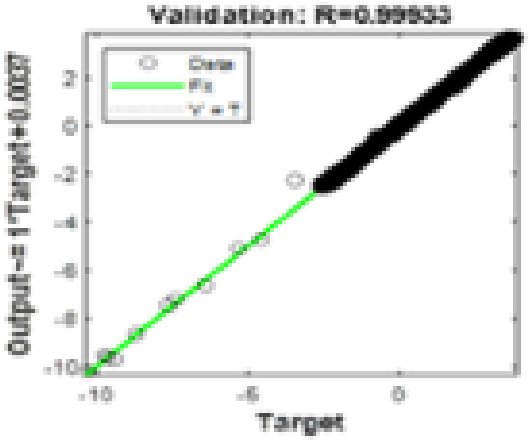

b)

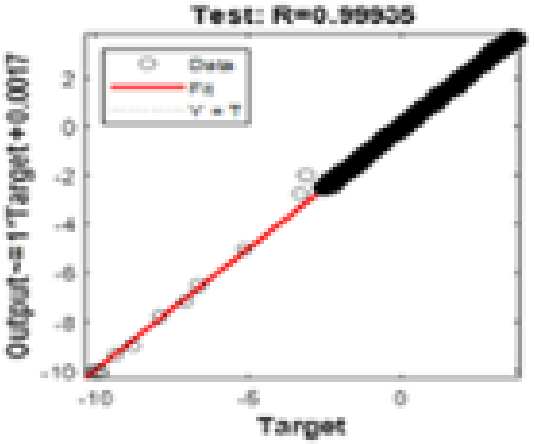

c)

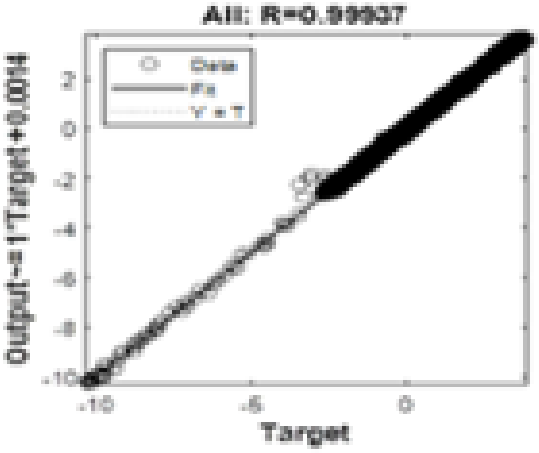

d)

Fig. 9. Datasets linear regressions: a) Training data regression; b) Validation data regression; c) Test data regression; d) Total data regression.

Subsequently, the temporary response obtained was evaluated by graphically relating the result of NARX network, against the required values. Fig. 10 shows the comparison between the results generated by each of datasets, against the target, in addition to

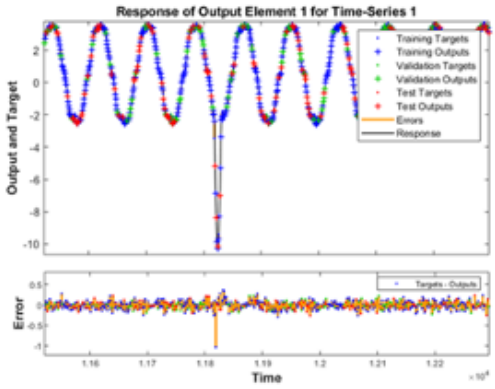

Fig. 10. Temporary response obtained and error, with respect to the objective.

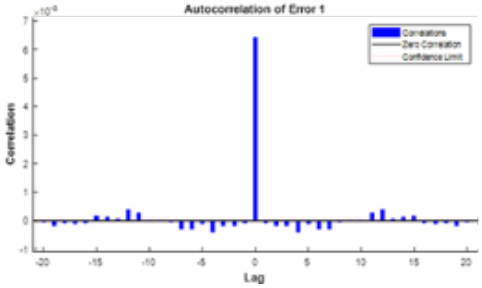

Fig. 11. Error-time autocorrelation.

the error present in each of moments of time. The response exhibits the characteristics of the difference between the current signal in the grid feeder in presence of power supplied by the PV system and the response obtained by the NARX, when entering the current signal from the electronic inverter to the PCC. From the errors' graph (Fig. 10), it is observed that the differences between the target values and those resulting from the three training datasets are very close to zero; showing the biggest errors when signal behavior exhibits rapid and abrupt changes in its waveform.

Finally, the correlation plots of errors with respect to time and inputs are displayed. Fig. 11, presents error-time autocorrelation; in it can be seen how the training is adequate; the central correlation (mse) with zero value, is greater, while the rest are within the expected confidence limits.

Fig. 12 shows the existence of a large number of correlations between inputs and error, which are within the limits; mostly concentrated in the zero value, so the training has optimal performance.

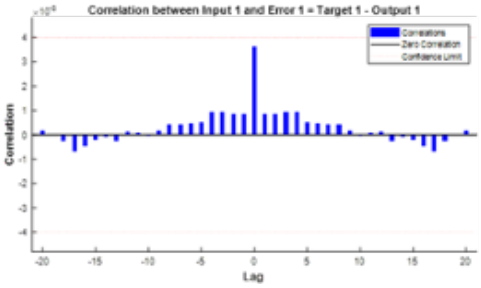

Fig. 12. Error-input correlation.

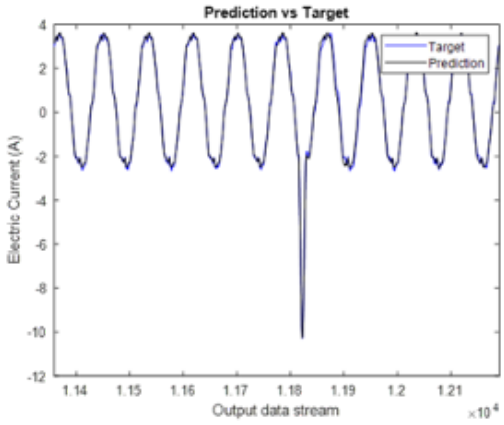

Fig. 13. Comparison of the temporal response of closed loop network against target output.

By replacing the configuration of the open-loop to closed-loop neural network (Fig. 6b), in such a way that, from the target inputs, the network uses its own predictions to check whether the model obtained through the open loop network has adequately defined the behavior of the current signal in the feeder of the electrical supply grid. This architecture produces results that differ from the temporal response of Fig. 10, and depend on how appropriate the training has been; but now, the target values will be unknown and the temporary response obtained will be the one shown in Fig. 13.

Fig. 14 shows the comparison of the output of the open loop network (model) against the target output. Similarity to Fig. 13 can be seen, small difference is being observed between the temporal response of the closed loop network and the open loop.

Table 2 shows the mse for each of the algorithms.

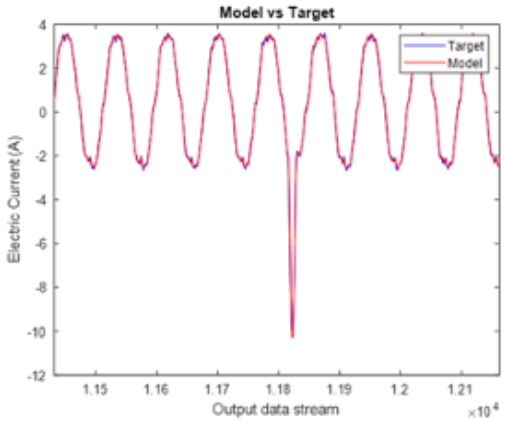

Fig. 14. Comparison of the temporary response of open loop network against target output.

Table 2. mse in modeling and prediction.

No.	Algorithm	mean squared error
1	Open loop NARX network (parallel-series)	0.0067
2	Closed loop NARX network (parallel)	0.0094

4 Discussion

Despite the results obtained with the use of deterministic analysis (shown in literature), these models do not give suitable results when trying to represent the behavior of non-stationary signals, due to the limitations presented by mathematical tools such as the transformed and Fourier series.

While ANNs have proven their efficiency when used for identification and classification processes, the ANN topologies used, have not been suitable for modeling and predicting time variant systems. With the application of the NARX network, the disadvantages that occur when analyzing non-stationary systems with deterministic methods based on the frequency domain were overcome, as well as extending the scope of such computational algorithms commonly used in the identification and classification of electrical loads and the harmonic distortion they produce.

On the other hand, the results of the application of the NARX network for modeling and predicting distorted current behavior in the supply grid, of dynamic characteristics are similar to the results obtained in the research that have used this same type of resource, in modeling and predicting the behavior of load current harmonics injected into energy micro-networks, as well as in the study of nonlinear high power loads.

Among the main advantages of this modeling methodology over others are:

1. Ability and ease to represent the nonlinear dynamics of the system,
2. Convergence with a small number of data with reduced computational time,
3. Suitability to represent internal dynamics through few input variables to the network,
4. Robustness for training-like conditions,
5. Simplicity in the use of the neural network.

Conclusions

At the end of the analysis of results, it was determined that the sinusoidal waveform of current in the electrical supply grid is affected, when integrated power from PV systems into the CCP through electronic inverters. Modeling the dynamic and nonlinear behavior of that signal using NARX networks, produce of a highly efficient pattern in terms of execution times, as well as computational resources, presenting a mse of 0.0067 with respect to the actual behavior of the signal; exhibiting a high performance of the neural network. The validity of the model was checked by forecasting the results, obtaining a mse of 0.0094 when using the closed loop NARX, showing a strong correlation between inputs and error values within the confidence limits.

Results suggests that a neural network with the appropriate characteristics may be considered suitable for capturing the dynamics of the harmonic current distortion in electrical grids, caused by the integration of power from PV systems. The obtained model presents great flexibility in terms of variety and amount of data that can be managed, allowing to represent and predict the behavior of the system under test in long periods and under various operating conditions. On the other hand, the resulting algorithm can be used for generation of physical or virtual systems that can be used for the control or reduction of harmonic phenomena affecting electrical grids.

References

Alhroob, E., Mohammed, M-F., Lim, C-P. and Tao, H. A. (2019). Critical review on selected fuzzy min-max neural networks and their significance and challenges in pattern classification. *IEEE Access 7*, 56129-56146. DOI: 10.1109/ACCESS.2019.2911955

Álvarez, C., Santana, G., Viveros, T. and Barrera, E. (2019). Efecto de los parámetros de depósito de silicio polimorfo por técnica PECVD sobre las propiedades químicas, nano-estructurales, optoelectrónicas y de foto-degradación. *Revista Mexicana de Ingeniería Química 16(3)*, 991-1001.

Bincy, K-J. (2017). Grid integration of PV systems-issues and requirements. *IEEE International Conference on Circuits and Systems (ICCS), Thiruvananthapuram, India*, 215-219. DOI: 10.1109/ICCS1.2017.8325993

Cortez, B., Carrera, B., Young-Jin, K. and Jae-Yoon, J. (2018) An architecture for emergency event prediction using LSTM recurrent neural networks. *Expert Systems with Applications 97*, 315-324. DOI: 10.1016/j.eswa.2017.12.037

Deng, Z., Rotaru, M-D, and Sykulski, J-K. (2017). Harmonic analysis of LV distribution networks with high penetration PV. *International Conference on Modern Power Systems (MPS), Cluj-Napoca, Romania*, 1-6. DOI: 10.1109/MPS.2017.7974392

Díaz, L., Hidalgo, C.A., Santoyo, E. and Hermosillo, J. (2020). Evaluación de técnicas de entrenamiento de redes neuronales para estudios geotermométricos de sistemas geotérmicos. *Revista Mexicana de Ingeniería Química 12(1)*, 105-120.

Figueroa, E., Farías, V.S., Segura, M., Andrade, I., Monter, M.I. and Chávez, A.M. (2020). Using artificial neural networks in prediction of the drying process of foods that are rich in sugars.

Revista Mexicana de Ingeniería Química 20(1), 161-171. DOI: 10.24275/RMIQ/SIM1403

Gómez, M.D., Hernández, I.A., López, J., González, G. and Beristain, R. (2020). Industrial wastewater treatment by anaerobic digestion using a solar heater as renewable energy for temperature-control. *Revista Mexicana de Ingeniería Química 19(1)*, 9-16. DOI: 10.24275/RMIQ/IA1853

Gupta, A-K., Pawar, V., Joshi, M. S., Agarwal V. and Chandran, D. A. (2017). Solar PV retrofit solution for residential battery inverters. *IEEE 44th Photovoltaic Specialist Conference (PVSC)*, Washington, DC, USA, 2986-2990. DOI: 10.1109/PVSC.2017.8366082

Hatata, A-Y. and Eladawy, M. (2017). Prediction of the true harmonic current contribution of nonlinear loads using NARX neural network. *Alexandria Engineering Journal 57(3)*, 1509-1518. DOI: 10.1016/j.aej.2017.03.050

Hudson M., Hagan, M., and Demuth, H. (2019). Matlab Deep Learning Toolbox User's Guide. *Mathworks*.

Javaid, N., Hafeez, G., Iqbal, S., Alrajeh, N., Alabed, M.S. and Guizani, M. (2018). Energy efficient integration of renewable energy sources in the smart grid for demand side management. *IEEE Access 6*, 77077-77096. DOI: 10.1109/ACCESS.2018.2866461

Kumar, N., Singh, B. and Panigrahi, B-K. (2019). Framework of gradient descent least squares regression-based NN structure for power quality improvement in PV-integrated low-voltage weak grid system. *IEEE Transactions on Industrial Electronics 66(12)*, 9724-9733. DOI: 10.1109/TIE.2018.2886765

Li, Y. and Cao, H. (2018). Prediction for tourism flow based on LSTM neural network. *Proceedings Computer Science 129*, 277-283. DOI: 10.1016/j.procs.2018.03.076

Liu, F., Chen, Z. and Wang, J. (2018). Video image target monitoring based on RNNLSTM. *Multimedia Tools and Applications 78*, 4527-4544, 2018. DOI: 10.1007/s11042-018-6058-6

Liu, Y., Rau, S., Wu, C., and Lee, W. (0218). Improvement of power quality by using advanced reactive power compensation. *IEEE Transactions on Industry Applications 54(1)*, 18-24. DOI: 10.1109/TIA.2017.2740840

Mejia, A., Amezquita, J-P., Dominguez, A., Valtierra, M., Razo, J-R. and Granados, D. (2017). A scheme based on PMU data for power quality disturbances monitoring. *IECON 2017 - 43rd Annual Conference of the IEEE Industrial Electronics Society, Beijing, China*, 3270-3275, DOI: 10.1109/IECON.2017.8216553

Mubarok, A-F., Octavira, T., Sudiharto, I., Wahjono, E., and Anggriawan, D-O. (2017). Identification of harmonic loads using fast fourier transform and radial basis Function Neural Network. *International Electronics Symposium on Engineering Technology and Applications (IES-ETA), Surabaya, Indonesia*, 198-202. DOI: 10.1109/ELECSYM.2017.8240402

Nduka, O-S. and Pal, B-C. (2016). Harmonic characterization model of grid interactive photovoltaic systems. *IEEE International Conference on Power System Technology (POWERCON), Wollongong, NSW, Australia*, 1-6. DOI: 10.1109/POWERCON.2016.7753863

Panoiu, M., Panoiu, C. and Ghiormez, L. (2018). Neuro-fuzzy modeling and prediction of current total harmonic distortion for high power nonlinear loads. *Innovations in Intelligent Systems and Applications (INISTA), Thessaloniki, Greece*, 1-7. DOI: 10.1109/INISTA.2018.8466290

Plangklang, B., Thanomsat, N. and Phuksamak, T. (2016). A verification analysis of power quality and energy yield of a large-scale PV rooftop. *Energy Reports 2*, 1-7. DOI: 10.1016/j.egyr.2015.12.002

Reinders, A., Debije, M. G. and Rosemann, A. (2017). Measured efficiency of a luminescent solar concentrator PV module called leaf roof. *IEEE Journal of Photovoltaics 7(6)*, 1663-1666, 2017. DOI: 10.1109/JPHOTOV.2017.2751513

Rezk, N-M., Purnaprajna, M., Nordstrom, T. and Ul-Abdin, Z. (2020). Recurrent neural networks: An embedded computing perspective. *IEEE*

Access 8, 57967-57996. DOI: 10.1109/ACCESS.2020.2982416

Rodriguez, M-A., Sotomonte, J-F., Cifuentes J. and Bueno, M. (2019). Classification of power quality disturbances using Hilbert Huang transform and a multilayer perceptron neural network model. *International Conference on Smart Energy Systems and Technologies (SEST), Porto, Portugal*, 1-6. DOI: 10.1109/SEST.2019.8849114

Salas, J., by Barros, F. and Martinez, F. (2019). Deep learning: Current state. *IEEE Latin America Transactions 17(12)*, 1925-1945. DOI: 10.1109/TLA.2019.9011537

Sangwongwanich A. and Blaabjerg, F. (2019). Mitigation of interharmonics in PV systems with maximum power point tracking modification. *IEEE Transactions on Power Electronics 34(9)*, 8279-8282. DOI: 10.1109/TPEL.2019.2902880

Shrestha, A. and Mahmood, A. (2019). Review of deep learning algorithms and architectures. *IEEE Access 7*, 53040-53065. DOI: 10.1109/ACCESS.2019.2912200

Shukl, P. and Singh, B. (2020). Delta-bar-delta neural-network-based control approach for power quality improvement of solar-PV-interfaced distribution system. *IEEE Transactions on Industrial Informatics 16(2)*, 790-801. DOI: 10.1109/TII.2019.2923567

Singh, S., Kewat, S., Singh, B., Panigrahi B. K. and Kushwaha, M. K. (2019). Seamless control of solar PV grid interfaced system with islanding pperation. *IEEE Power and Energy Technology Systems Journal 6(3)*, 162-171. DOI: 10.1109/JPETS.2019.2929300

Todeschini, G., Balasubramaniam, S. and Petar Igic (2019). Time-domain modeling of a distribution system to predict harmonic interaction between PV converters. *IEEE Transactions on Sustainable Energy 10(3)*, 1450-1458. DOI: 10.1109/TSTE.2019.2901192

Vargas, U., Ramirez, A., and Lazaroiu, G-C. (2017). Flexible harmonic domain model of a photovoltaic system for steady-state analysis. *International Conference on Energy and Environment (CIEM), Bucharest, Romania*, 311-315. DOI: 10.1109/CIEM.2017.8120805

Xia, W., Zhu, W., Liao, B., Chen, M., Cai, L. and Huang, L. (2018). Novel architecture for long short-term memory used in question classification. *Neurocomputing 299*, 20-31, 2018. DOI: 10.1016/j.neucom.2018.03.020